

## Supplementary Information

### Supramolecular Regulation of Bioorthogonal Catalysis in Cells Using Nanoparticle-Embedded Transition Metal Catalysts

Gulen Yesilbag Tonga<sup>†</sup>, Youngdo Jeong<sup>†</sup>, Bradley Duncan, Tsukasa Mizuhara, Rubul Mout, Riddha Das, Sung Tae Kim, Yi-Cheun Yeh, Bo Yan, Singyuk Hou, and Vincent M. Rotello\*

Department of Chemistry, University of Massachusetts, 710 North Pleasant Street, Amherst, Massachusetts 01003, USA.

\* Corresponding authors:

Vincent M. Rotello

Email: rotello@chem.umass.edu

Phone: (+1) 413-545-2058

Fax: (+1) 413-545-4490

<sup>†</sup>These authors contributed equally to this work.

### Synthesis of the benzyl ligand

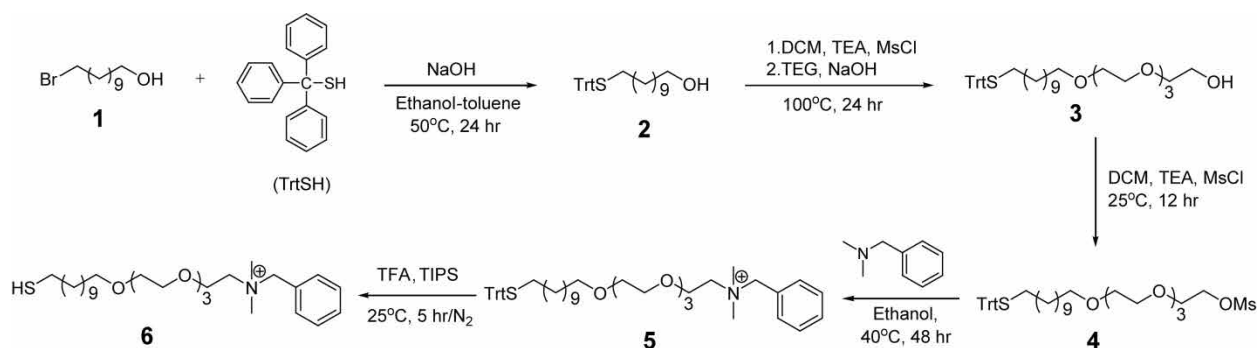


**Figure S1.** Synthetic scheme of the benzyl ligand for the functionalization of the nanoparticle.

## General procedure:

**Compound 2:** 11-bromo-1-undecanol (1, 10 g, 39.8 mmol) was dissolved in 1:1 ethanol/toluene mixture (200 ml). Triphenylmethanethiol (13.2 g, 47.77 mmol) dissolved in 1:1 ethanol/toluene (50 ml) was added to 11-bromo-1-undecanol in solution. Then NaOH (2.38 g, 59.7 mmol) dissolved in 3 ml water was slowly added to the mixture. The reaction mixture was stirred for 24 h at 50°C. Upon completion, the reaction mixture was extracted with a saturated solution of NaHCO<sub>3</sub> twice. The organic layer was extracted, dried over Na<sub>2</sub>SO<sub>4</sub>, and concentrated by evaporation of the solvent. The crude product was purified by column chromatography over silica gel using hexane/ethyl acetate (1:1, v/v) as the eluent. The solvent was removed in vacuum to obtain compound **2** as colorless oil (Yield 16.42 g, 92%).

**<sup>1</sup>H NMR (400 MHz, CDCl<sub>3</sub>, TMS) of Compound 2 :**  $\delta$  7.48-7.40 (m, 6H, *H*Ar-), 7.37-7.27 (m, 6H, *H*Ar-), 7.26-7.18 (m, 3H, *H*Ar-), 3.65 (t, *J* = 6.7Hz, 2H, **CH**<sub>2</sub>OH), 2.16 (t, *J* = 7.2Hz, 2H, -**CH**<sub>2</sub>-), 1.66-1.52 (m, 2H, -S**CH**<sub>2</sub>**CH**<sub>2</sub>), 1.44-1.12 (m, 16H, -**CH**<sub>2</sub>CH<sub>2</sub>OH + -(**CH**<sub>2</sub>)<sub>8</sub>CH<sub>2</sub>OH).

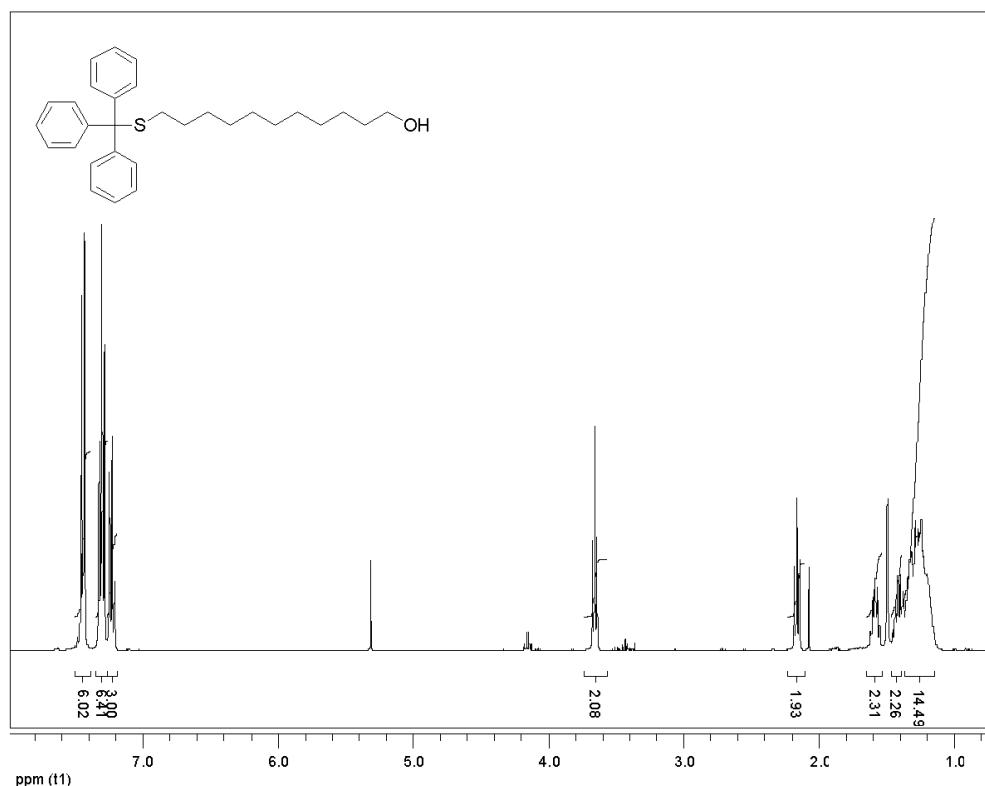


**Figure S2.** <sup>1</sup>H NMR spectrum (400 MHz) of compound 2 in CDCl<sub>3</sub> (D, 99.8%).

**Compound 3:** Compound **2** (16.42 g, 36.76 mmol) in dry dichloromethane (DCM, 200 ml) was mixed with triethylamine (5.58 g, 7.66 mL, 55.14 mmol), followed by dropwise addition of methanesulfonyl chloride (4.64 g, 3.13 mL, 40.47 mmol) in ice bath. After 30 min the reaction mixture was warmed up to room temperature and stirred overnight. After the reaction was completed (according to thin layer chromatography; TLC), solvent was evaporated. The compound was again diluted with DCM and extracted with 0.1 M HCl twice. The organic layer was collected, treated with a saturated solution of NaHCO<sub>3</sub>, and washed three times. Following extraction, the organic layer was dried over Na<sub>2</sub>SO<sub>4</sub> and concentrated at reduced pressure. The crude product was purified by column chromatography over silica gel using hexane/ethyl acetate (1:1, v/v) as the eluent. Solvent was removed in vacuum to obtain mesylated compound as light yellow oil (Yield 17.4 g, 90%). To synthesize compound **3**, NaOH (1.59 g, 39.8 mmol) solution (1.5 mL) was added to 115 mL of tetraethyleneglycol (128.93 g, 66.37 mmol) and stirred for 2 h at 80°C. To this reaction mixture, 17.4 g of 11-(tritylthio)undecyl methanesulfonate (30.03 mmol) was added and stirred for 24 h at 100°C. The product was extracted in hexane/ethyl acetate (100 ml, 4:1, v/v) six times. Then, the organic layer was concentrated at reduced pressure and the crude product was purified by column chromatography over silica gel using ethyl acetate as the eluent. The solvent was removed in vacuum to obtain compound **3** as light yellow oil (Yield 11.6 g, 62%).

**<sup>1</sup>H NMR (400 MHz, CDCl<sub>3</sub>, TMS) of Compound 3:** δ 7.47-7.40 (m, 6H, *HAr*-), 7.34-7.26 (m, 6H, *HAr*-), 7.25-7.19 (m, 3H, *HAr*-), 3.77-3.57 (m, 16H, -CH<sub>2</sub>-(OCH<sub>2</sub>CH<sub>2</sub>)<sub>4</sub>-OH), 3.46 (t, *J* = 6.8 Hz, 2H, -CH<sub>2</sub>-(OCH<sub>2</sub>CH<sub>2</sub>)<sub>4</sub>-OH), 2.95 (br, s, 1H, -TEG-OH), 2.15 (t, *J* = 7.2 Hz, -SCH<sub>2</sub>-), 1.59 (p, *J* = 7.2 Hz, 2H, -CH<sub>2</sub>CH<sub>2</sub>TEG-OH), 1.4 (p, *J* = 7.6 Hz, 2H, -SCH<sub>2</sub>CH<sub>2</sub>-), 1.35-1.13 (m, 14H, -(CH<sub>2</sub>)<sub>7</sub>CH<sub>2</sub>CH<sub>2</sub>TEG-OH).

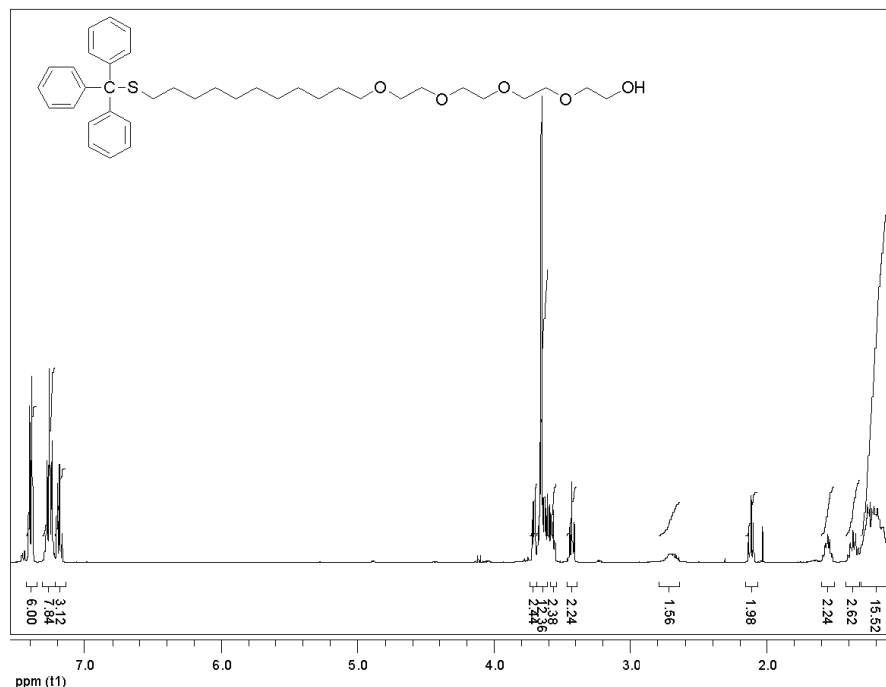


**Figure S3.**  $^1\text{H}$  NMR spectrum (400 MHz) of compound 3 in  $\text{CDCl}_3$  (D, 99.8%).

**Compound 4:** Triethylamine (2.6 g, 3.6 mL, 25.6 mmol) was added to compound 3 (8 g, 12.8 mmol) in dry DCM (80 ml) in an ice bath. Methanesulfonyl chloride (2.22 g, 1.49 mL, 19.28 mmol) was added dropwise to the reaction mixture in an ice bath. After 30 min the reaction mixture was warmed up to room temperature and stirred 12 h. The organic layer was extracted twice with a saturated solution of  $\text{NaHCO}_3$  (100 ml) and twice with 0.1 M HCl solution (100 ml). The extracted DCM layer was dried over  $\text{Na}_2\text{SO}_4$  and concentrated at reduced pressure. The crude product was purified by column chromatography over silica gel using ethyl acetate as the eluent. Solvent was removed in vacuum to obtain compound 4 as light yellow oil (Yield 8.2 g, 91 %).

**$^1\text{H}$  NMR (400 MHz,  $\text{CDCl}_3$ , TMS) of Compound 4:**  $\delta$  7.44-7.37 (m, 6H, *HAr*-), 7.31-7.23 (m, 6H, *HAr*-), 7.22-7.16 (m, 3H, *HAr*-), 4.40-4.34 (m, 2H,  $-\text{CH}_2\text{OSO}_3\text{CH}_3$ ), 3.78-3.54 (m, 14H,  $\text{CH}_2-(\text{OCH}_2\text{CH}_2)_3-\text{CH}_2\text{CH}_2\text{OSO}_3\text{CH}_3$ ), 3.44 (t,  $J = 6.8\text{Hz}$ , 2H,  $\text{CH}_2-\text{CH}_2-(\text{OCH}_2\text{CH}_2)_3-$ ), 3.07 (s, 3H,  $-\text{OSO}_3\text{CH}_3$ ), 2.12 (t,  $J = 7.2\text{Hz}$ , 2H,  $-\text{SCH}_2-$ ), 1.56 (p,  $J = 7.2\text{Hz}$ , 2H,  $-\text{CH}_2\text{CH}_2\text{TEG}-\text{N}(\text{CH}_3)_2$ ), 1.38 (p,  $J=7.6\text{Hz}$ , 2H,  $-\text{SCH}_2\text{CH}_2-$ ), 1.32-1.11 (m, 14H,  $-(\text{CH}_2)_7\text{CH}_2\text{CH}_2\text{TEGOSO}_3\text{CH}_3$ ).

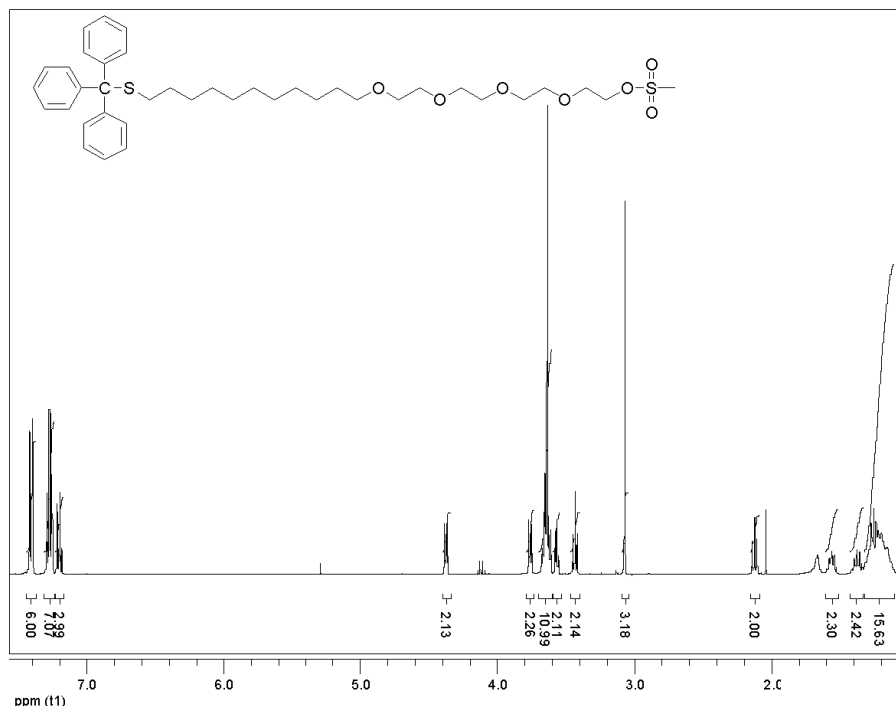


**Figure S4.**  $^1\text{H}$  NMR spectrum (400 MHz) of compound 4 in  $\text{CDCl}_3$  (D, 99.8%).

**Compound 5:** Compound 4 (1 g, 1.42 mmol) was added to dimethylbenzylamine (0.58 g, 0.65 ml, 4.28 mmol) in ethanol-DCM mixture (4:1, v/v, 5 ml). The reaction mixture was stirred at  $40^\circ\text{C}$  for 48 h. After evaporating ethanol at reduced pressure, the light yellow residue was purified by successive washings with hexane (four times) and hexane/diethylether (1:1 v/v, six times) and then dried under high vacuum. The product formation was around 100% and the product was confirmed by NMR.

**$^1\text{H}$  NMR (400MHz,  $\text{CDCl}_3$ , TMS) of Compound 5:**  $\delta$  7.64-7.58 (m, 2H, *HAr*-), 7.38-7.32 (m, 9H, *HAr*-), 7.24-7.17 (m, 6H, *HAr*-), 7.16-7.09 (m, 3H, *HAr*-), 4.9 (s, 2H,  $-\text{CH}_2-\text{C}_6\text{H}_5$ ), 3.94 (s, br, 2H,  $-\text{OCH}_2\text{CH}_2\text{N}(\text{CH}_3)_2$ -), 3.8 (s, br, 2H,  $-\text{OCH}_2\text{CH}_2\text{N}(\text{CH}_3)_2$ -), 3.77-3.22 (m, 12H,  $-(\text{OCH}_2\text{CH}_2)_3-\text{CH}_2\text{CH}_2\text{N}(\text{CH}_3)_2$ -), 3.33 (t,  $J = 6.8\text{Hz}$ , 2H,  $-\text{CH}_2\text{CH}_2\text{O}-$ ), 3.23 (s, 6H,  $-\text{N}(\text{CH}_3)_2$ -), 2.06 (t,  $J = 7.2\text{Hz}$ , 2H,  $-\text{SCH}_2$ -), 1.51-1.42 (p,  $J = 6.8\text{Hz}$ , 2H,  $-\text{CH}_2\text{CH}_2\text{O}-$ ), 1.36-1.28 (p,  $J = 7.6\text{Hz}$ , 2H,  $-\text{SCH}_2\text{CH}_2$ -), 1.24-1.08 (m, 14H,  $-(\text{CH}_2)_7\text{CH}_2\text{CH}_2\text{O}-$ ).

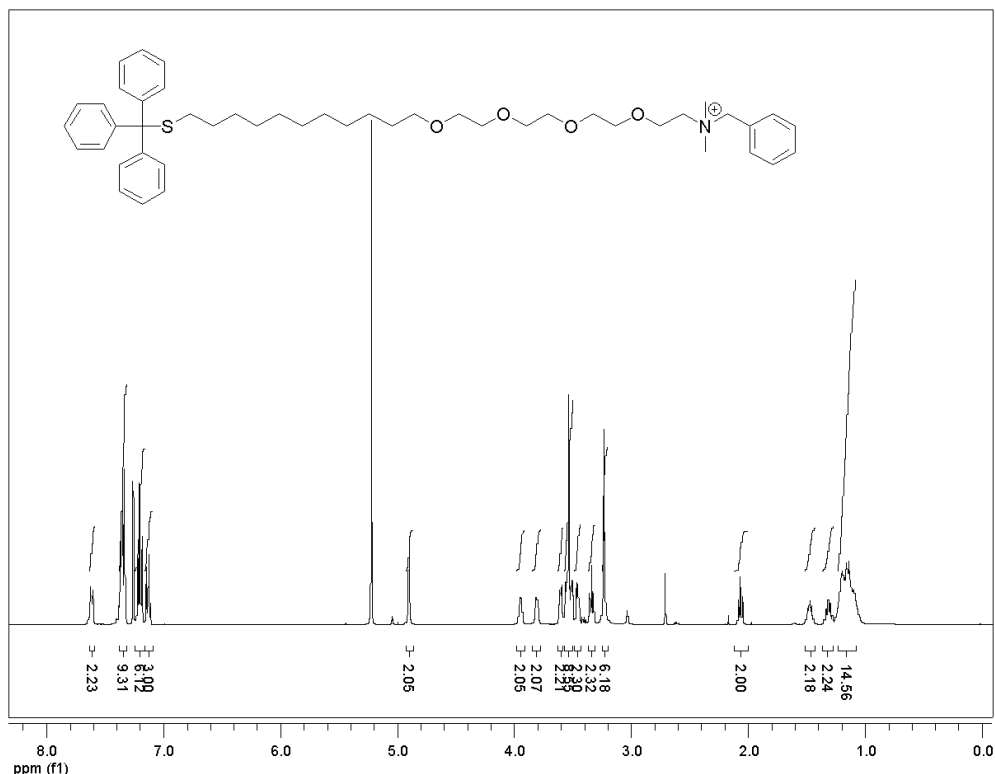


**Figure S5.**  $^1\text{H}$  NMR spectrum (400 MHz) of compound **4** in  $\text{CDCl}_3$  (D, 99.8%).

**Compound 6:** An excess of trifluoroacetic acid (TFA, 20 equivalents, 3.07 g, 2.08 mL, 27 mmol) was added to compound **5** (1 g, 1.12 mmol) in dry DCM (5 ml). The color of the solution was turned to yellow-orange upon addition of TFA. Then, triisopropylsilane (TIPS, three equivalents, 0.64g, 0.83 mL, 4.05 mmol) was added to the reaction mixture and the color of the solution turned to clear. The reaction mixture was stirred 5 hr under  $\text{N}_2$  at room temperature. The solvent, most of TFA, and TIPS were evaporated under reduced pressure. The yellow residue was purified by hexane washings (four times) and dried under high vacuum. The final product formation was around 100% and the structure of compound **6** was confirmed by NMR.

$^1\text{H}$  NMR (400 MHz,  $\text{CDCl}_3$ , TMS) of Compound **6**:  $\delta$  7.57-7.47 (m, 5H), 4.61 (s, 2H,  $-\text{CH}_2-\text{C}_6\text{H}_5$ ), 4.01 (s, br, 2H,  $-\text{OCH}_2\text{CH}_2\text{N}(\text{CH}_3)_2-$ ), 3.74-3.48 (m, 14H,  $-(\text{OCH}_2\text{CH}_2)_3-\text{CH}_2\text{CH}_2\text{N}(\text{CH}_3)_2-$ ), 3.41 (t,  $J = 6.8\text{Hz}$ , 2H,  $-\text{CH}_2\text{CH}_2\text{O}-$ ), 3.14 (s, 6H,  $-\text{N}(\text{CH}_3)_2-$ ), 2.52 (q,  $J = 7.2\text{Hz}$ ,  $\text{HSCH}_2-$ ), 1.65-1.48 (m, 4H,  $-\text{CH}_2\text{CH}_2\text{O}- + \text{HSCH}_2\text{CH}_2-$ ), 1.43-1.20 (m, 15H,  $-(\text{CH}_2)_7\text{CH}_2\text{CH}_2\text{O}- + \text{HS}-$ ).

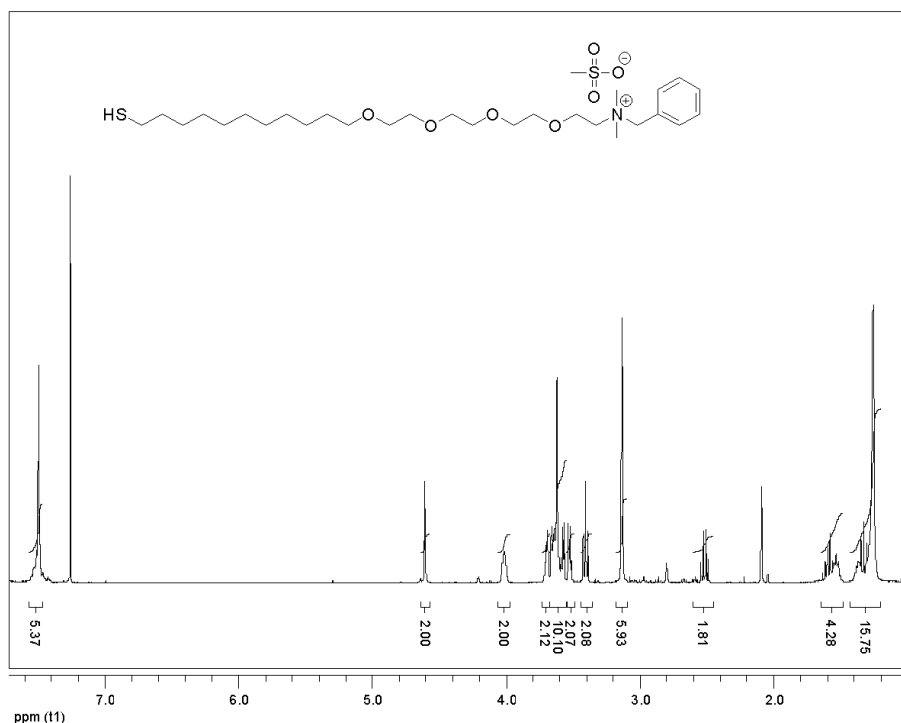


**Figure S6.**  $^1\text{H}$  NMR spectrum (400 MHz) of benzyl ligand in  $\text{CDCl}_3$  (D, 99.8%).

### Synthesis of benzyl-ligand-protected gold nanoparticle (AuNP)

First, Brust-Schiffrin two-phase synthesis method was used to synthesize pentanethiol-coated AuNPs with core diameter ca. 2 nm<sup>1,2</sup>. Murray place-exchange method<sup>3</sup> was followed to obtain the benzyl-ligand-protected AuNPs. Pentanethiol-conjugated AuNPs (10 mg) and thiol ligand (compound **5**) (30 mg) were dissolved in a mixture of dry DCM (3 ml) and methanol (1 ml) and stirred under  $\text{N}_2$  atmosphere for 3 days at room temperature. The DCM was removed under reduced pressure and the resulting precipitate was washed with hexane (15 ml) three times and DCM (15 ml) twice. Then the precipitate was dissolved in distilled water (~ 5 ml) and dialyzed for three days (membrane molecular weight cut-off =10,000, volume of the dialysis bucket is 5 L) to remove excess ligands, pentanethiol, acetic acid, and other salts present in the nanoparticle solution. After dialysis, the particle was lyophilized to yield a solid brownish product. The particles were then re-dispersed in deionized water.  $^1\text{H}$  NMR-spectra in  $\text{D}_2\text{O}$  showed substantial broadening of the proton peaks with no sign of free ligands. The presence of ligands was also confirmed by mass spectroscopy.

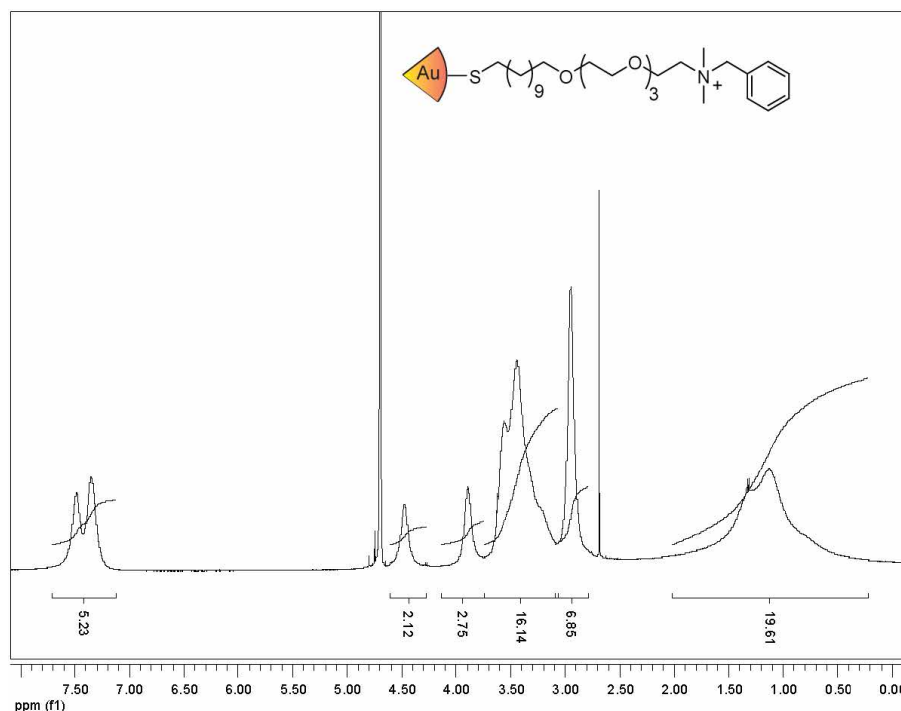


**Figure S7.**  $^1\text{H}$  NMR spectrum (400 MHz) of benzyl-AuNPs in  $\text{D}_2\text{O}$  (D, 99.8%).

### Mass spectrometric characterization of ligand composition

Matrix assisted laser desorption/ionization mass spectroscopy (MALDI-MS) has been performed to characterize the surface ligand on the Benzyl-AuNP<sup>4</sup>. A saturated  $\alpha$ -Cyano-4-hydroxycinnamic acid ( $\alpha$ -CHCA) stock solution was prepared in 70% acetonitrile, 30%  $\text{H}_2\text{O}$ , and 0.1% trifluoroacetic acid. An equal volume of 2  $\mu\text{M}$  NP solution was added to the matrix stock solution. 2.5  $\mu\text{L}$  of this mixture was applied to the sample carrier, and then the MALDI-MS analysis was performed on a Bruker Autoflex III mass spectrometer. The molecular ions ( $\text{MH}^+$ ,  $m/z = 498$ ) was detected, and the disulfide ion formed by the benzyl ligand and the original pentanethiol was also detected at  $m/z$  600.



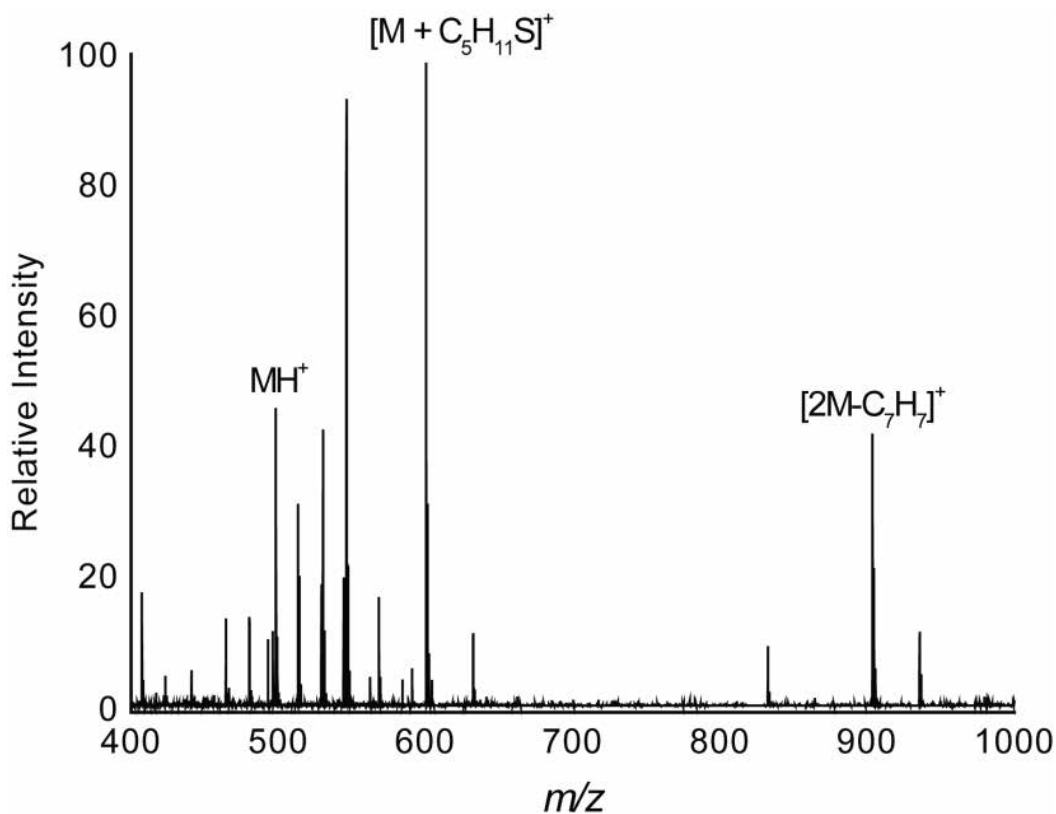


Figure S8. MALDI-MS spectrum of benzyl-AuNP.

### Transmission electron microscopy (TEM) measurement of the nanoparticle before and after the encapsulation of the catalysts

TEM samples of AuNP and  $[Cp^*Ru(cod)Cl]$  catalysts encapsulated AuNP were prepared by placing one drop of the desired solution ( $1 \mu M$ ) on to a 300-mesh Cu grid-coated with carbon film. These samples were analyzed and photographed using JEOL CX-100 electron microscopy. The average diameter of Au core is  $2.5 \pm 0.4$  nm.

### Catalyst encapsulation into the monolayer of AuNPs

3 mg of the catalyst,  $[Cp^*Ru(cod)Cl]$  or (1,1'- Bis(diphenylphosphino)ferrocene)palladium(II)dichloride was dissolved in 5 ml acetone and the AuNP ( $20 \mu M$ , 0.5 mL) were diluted to a final concentration of  $5 \mu M$  with DI water (2 ml). Then, the catalyst and the AuNP solutions were mixed together and acetone was slowly removed by evaporation. During the evaporation hydrophobic catalyst was encapsulated in the particle monolayer to yield to **NP\_Ru** or **NP\_Pd**. Excess

catalysts which precipitated in water removed by filtration (Millex-GP filter; 25 mm PES, pore Size: 0.22 $\mu$ m). Further purifications were followed by multiple filtrations (five times, Amicon<sup>®</sup> ultra 4, 10K) and dialysis (Snake Skin<sup>®</sup> dialysis tubing, 10K) against water (5 L) for 24 h to remove free catalysts. The amount of encapsulated catalysts was measured by ICP-MS by tracking <sup>101</sup>Ru relative to <sup>197</sup>Au for **NP\_Ru** and <sup>106</sup>Pd relative to <sup>197</sup>Au for **NP\_Pd**.

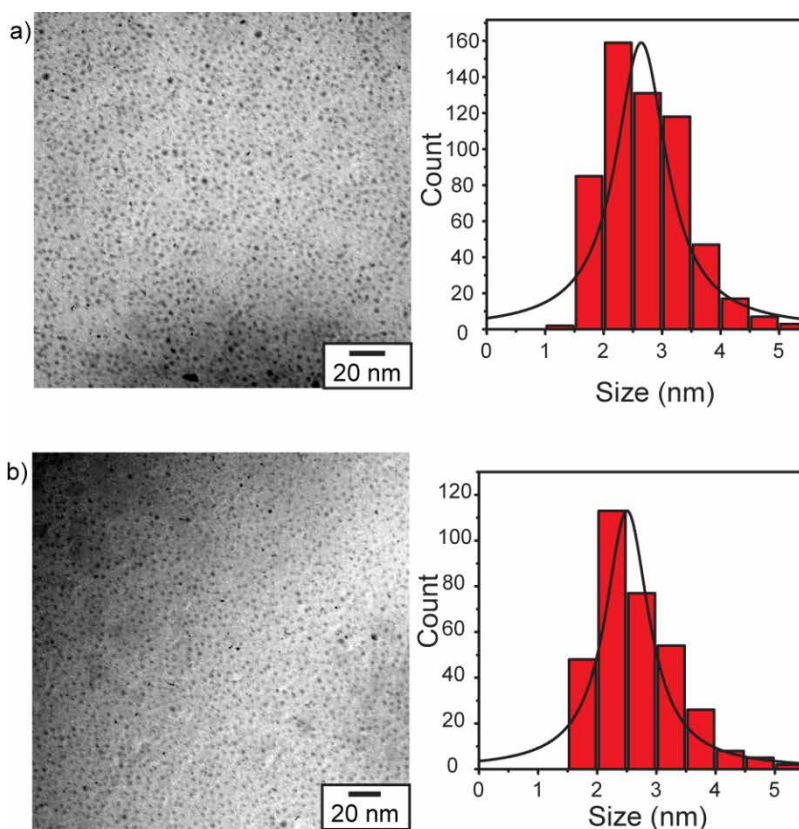


**Figure S9.** TEM images of AuNP with (a) without (b) encapsulation of the ruthenium catalysts. No size change or aggregation of nanoparticles was observed from TEM images, indicating no morphological change occurred during encapsulation process.

### Size and zeta potential of the NP

Hydrodynamic diameter and zeta potential of the NPs were measured by dynamic light scattering (DLS) in DI water and 5 mM phosphate buffer (pH=7.4) respectively, using a Malvern Zetasizer Nano ZS instrument. The measurement angle was 173<sup>°</sup> (backscatter). Data were analyzed by the “multiple narrow modes” (high resolution) based on non-negative-least-squares (NNLS).

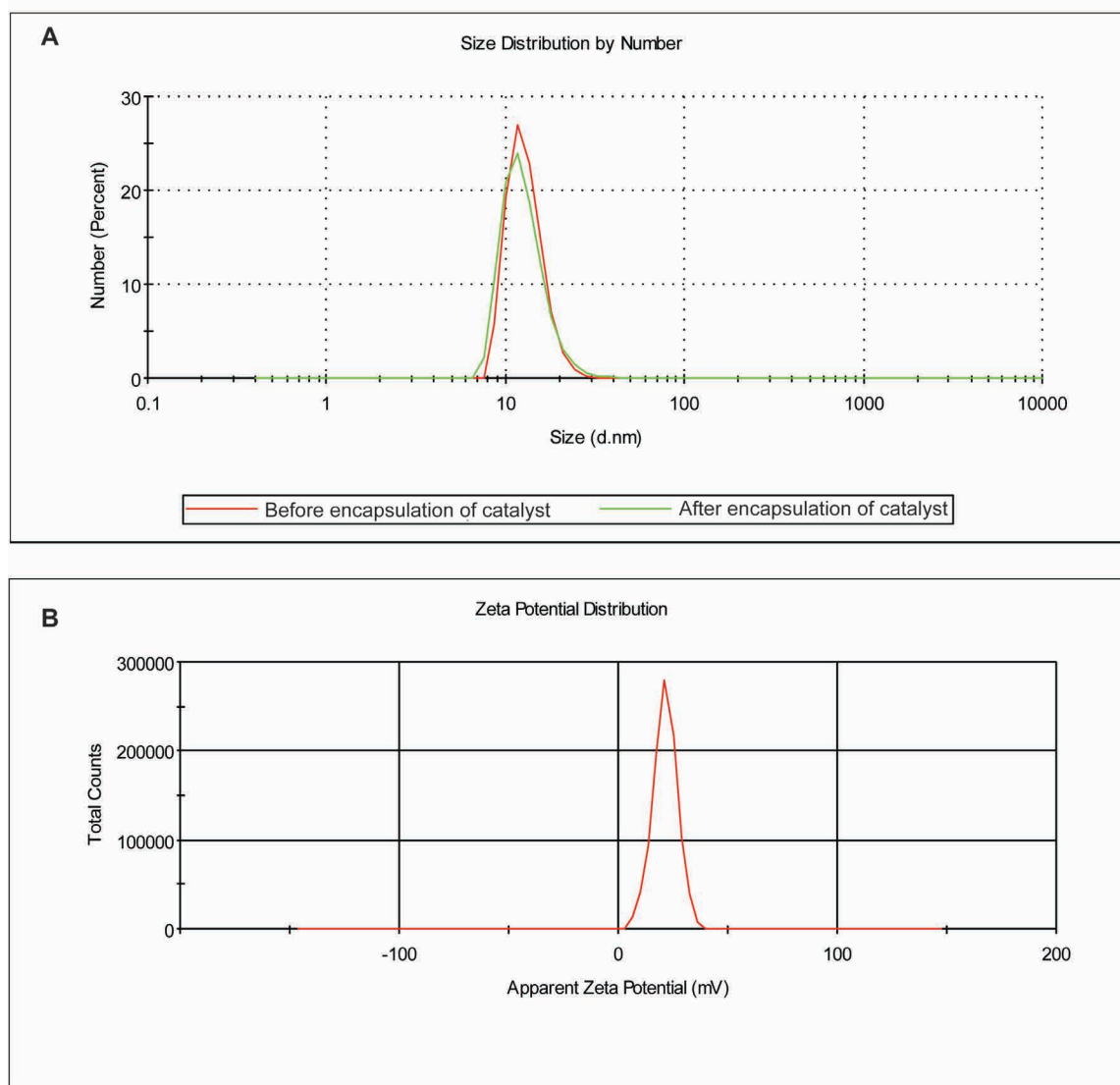


**Figure S10.** Characterization of the functionalized AuNP. a, Size (diameter) of AuNP was measured by DLS before and after catalyst encapsulation. DLS measurement shows that size of the NP after catalyst encapsulation stays same. b, Zeta potential of AuNP was measured by DLS. The overall charge of AuNP is measured as  $25.5 \pm 1$  mV from three independent replicates.

## Inductively coupled plasma mass spectrometry (ICP-MS) instrumentation

The ICP-MS analyses were performed on a Perkin-Elmer NexION 300X ICP mass spectrometer.  $^{197}\text{Au}$  and  $^{101}\text{Ru}$  were measured under the standard mode. Operating conditions are listed as below: nebulizer flow rate: 0.95 L/min; rf power: 1600 W; plasma Ar flow rate: 18 L/min; dwell time: 50 ms. Standard gold and ruthenium solutions (concentration: 0, 0.2, 0.5, 1, 2, 5, 10, and 20 ppb) were prepared for the quantification.

## ICP-MS sample preparation for the quantification of gold and ruthenium

0.5 mL of fresh *aqua regia* was added to the 10  $\mu\text{L}$  sample solution and then the sample was diluted to 10 mL with de-ionized water.

	Au	Ru	Ru ppb	Ru (ng)	Ru (ng)/ AuNP(pmol)	Ru (pmol) / AuNP(pmol)
Sample 1	141305.705	22536.207	0.41264275	4.27167771	4.50	44.55
Sample 2	150104.223	20097.671	0.36470407	3.7388732	3.94	39.01
Sample 3	149605.987	21269.236	0.38773563	3.9023652	4.20	41.58
				Average	4.21	41.72
				S.D.	0.28	2.77

**Figure S11.** Ruthenium amount in the nanozyme using ICP-MS measurement.

## Catalytic activity of the nanozymes inside vial

Catalytic activities of **NP\_Ru** and **NP\_Ru\_CB[7]** were tested in vials. 400 nM of **NP\_Ru** and 400 nM of **NP\_Ru\_CB[7]** (2 ml in DI water) were mixed with 5  $\mu\text{L}$  of caged rhodamine 110 substrate (20 mM in DMSO) for 24 h at room temperature. Fluorescence was observed using the nanozymes (**NP\_Ru**) while only little fluorescence was observed with the **NP\_Ru\_CB[7]** (Figure S12). This background fluorescence was coming from the caged-fluorophore itself as shown

in Figure S12 taken at 0 h (Figure S13).

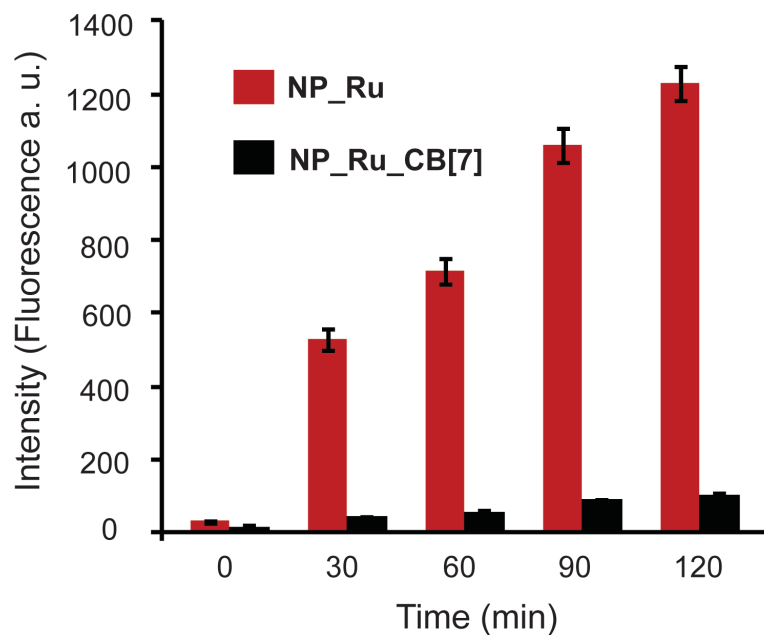


**Figure S12.** Bar graph of intensities of **NP\_Ru** and **NP\_Ru\_CB[7]** at 5 different time points for 2 h.

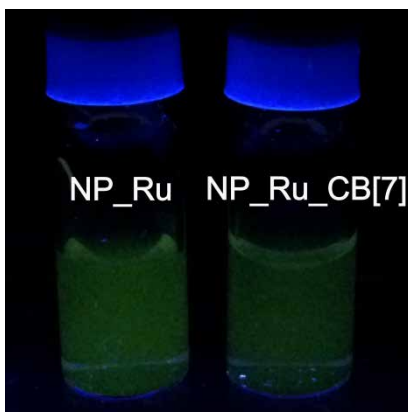


**Figure S13.** Photo of the reaction mixtures in water with **NP\_Ru** and **NP\_Ru\_CB[7]** under UV light at 0 h.

### Catalytic activity of the nanozyme versus NP inside vial

Catalytic activities of **NP\_Ru** and only **NP** were tested in vials. 400 nM of **NP\_Ru** and 400 nM of **NP** (2 ml in DI water) were mixed with 5  $\mu$ L of caged rhodamine 110 substrate (20 mM in DMSO) for 24 h at room temperature. Fluorescence was observed using the nanozymes (**NP\_Ru**) while no fluorescence was observed with the control particle **NP** that lacked embedded catalysts.

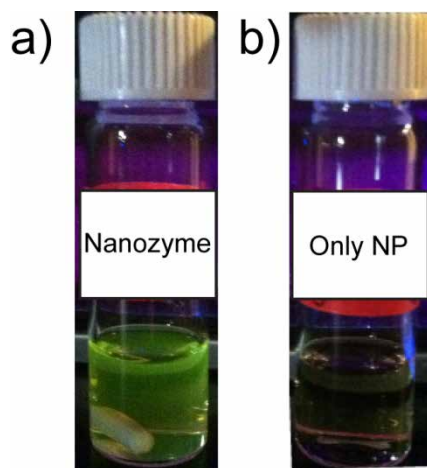


**Figure S14.** Reaction mixtures including a, the nanozyme and caged rhodamine 110 and b, AuNP and caged rhodamine 110 after 24 h.

### Long term stability of nanozymes

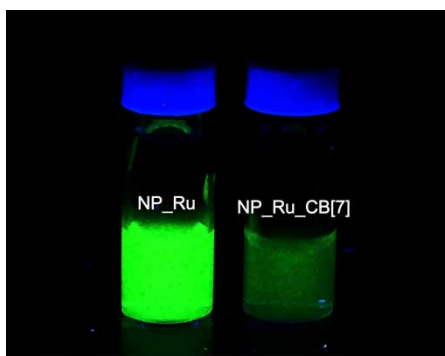


**Figure S15.** Photo of the reaction mixtures in water with NP\_Ru and

NP\_Ru\_CB[7] under UV light after 5 days.

### ITC measurement

MicroCal™ VP-ITC System was used for ITC measurements. Experiments were performed by titrating CB[7] solution in water (2 mM, 170  $\mu$ L) into AuNP solution in water (1  $\mu$ M, 1.8 mL). Cell temperature was adjusted to 30°C and injection parameters were as follows: volume: 3  $\mu$ L, duration: 6 sec, spacing: 180 sec, filter period: 2 sec.

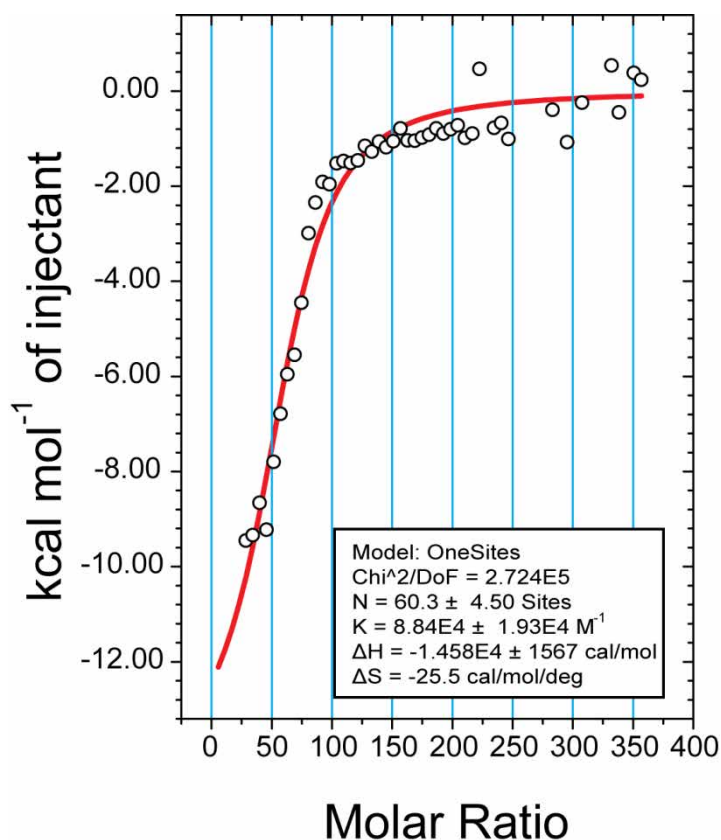


**Figure S16.** ITC titration of CB[7]s into the NP solution. The circles represent the integrated heat changes during complex formation and the lines represent the curve fit to the binding isotherm.

### Catalytic activities of free catalysts in water/acetone mixture in the presence of CB[7] or CB[7] + ADA

1  $\mu$ l of the caged rhodamine 110 substrate stock solution (20 mM in DMSO) was added in Cp\*Ru(cod)Cl catalyst solution (1.5  $\mu$ M in 1 ml water/acetone (1:1, v:v)). Reactions were monitored for 5 min by tracking the absorbance at 500 nm using

the UV-visible spectrometer (SpectraMax M2).

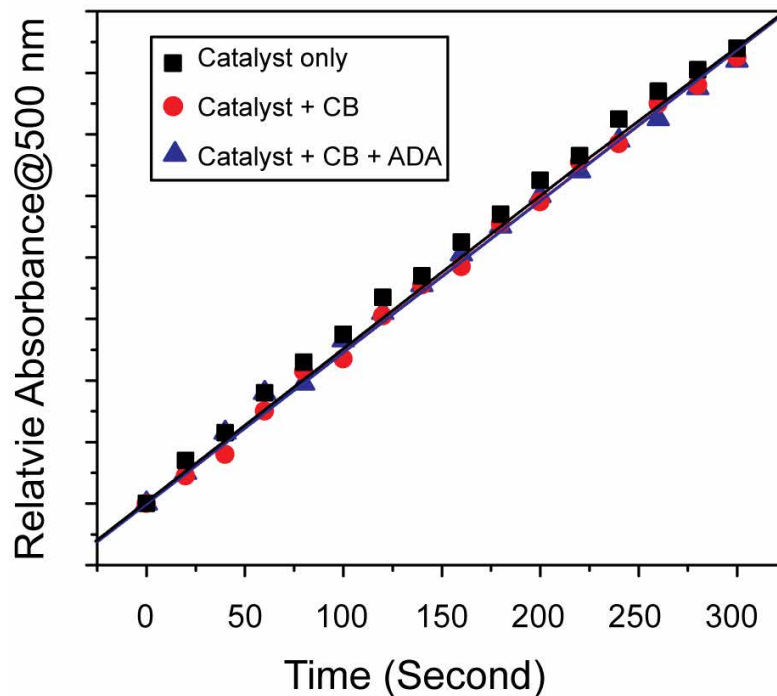


**Figure S17.** Activity assay of allylcarbamate cleavage of the  $[\text{Cp}^*\text{Ru}(\text{cod})\text{Cl}]$  in acetone/water (1:1 v/v). No catalytic activity change was observed in presence of CB[7] or CB[7] + ADA, indicating CB[7] or ADA cannot affect the catalytic activity of the catalysts directly.

### Lineweaver-Burk analysis

To monitor the inhibition mechanism of the nanozymes, the catalytic reactions of the nanozymes were carried out in sodium phosphate buffer (5 mM, pH 7.4). In the activity studies, the nanozyme (400 nM) was mixed with various concentrations of substrates (2, 4, 20, 40, 80  $\mu\text{M}$ ) and CB[7]s (0, 4, 16, 80  $\mu\text{M}$ ) in a 96-well plate, and the final volume for each well was 250  $\mu\text{L}$ . The catalytic activity was monitored by tracking the fluorescence intensity (Ex: 488 nm, Em: 521 nm, Cutoff: 515 nm) using a Molecular Devices SpectraMax M2 microplate reader. The concentrations of products were obtained from the fluorescence intensity and the fluorescence standard curve (Figure S30).



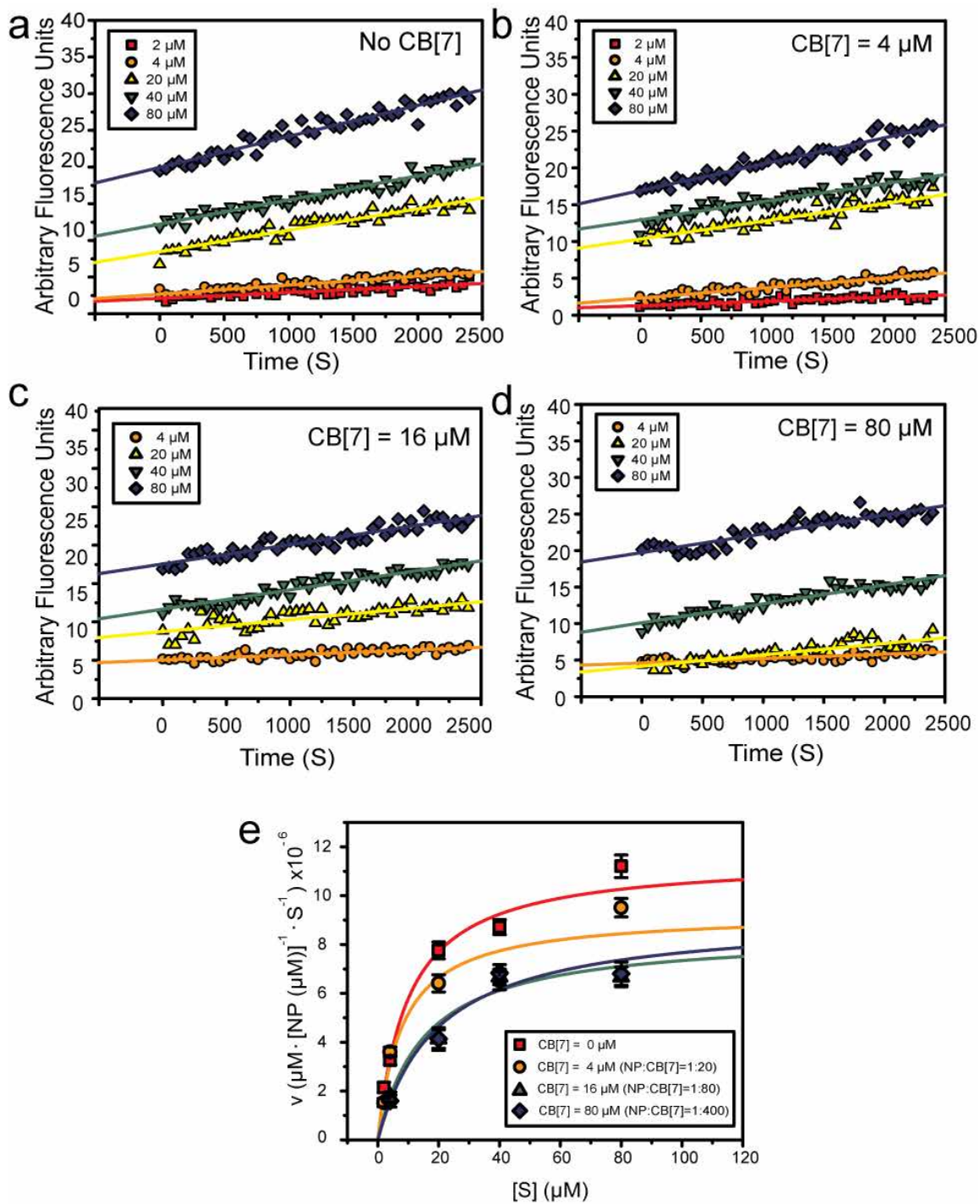


**Figure S18.** The dependence of reaction rates on the concentration of the CB[7] (a, 0  $\mu\text{M}$ ; b, 4  $\mu\text{M}$ ; c, 16  $\mu\text{M}$ ; and d, 80  $\mu\text{M}$ ). e, The fitting curve of the reaction rate vs. concentration of the substrates.

## Reaction rates titration for the nanozymes

The reaction rates of the nanozymes were titrated by increasing the concentration of CB[7]. The catalytic reactions of the nanozymes were carried out in sodium phosphate buffer (5 mM, pH 7.4). In the activity studies, the nanozyme (400 nM) was mixed with substrate solution (80  $\mu$ M) in a 96-well plate. To titrate the catalytic activity, CB[7]s (0, 4, 8, 16, 32, 64, 80, 100  $\mu$ M), were added and the final volume for each well was 250  $\mu$ L. The catalytic activity was monitored by tracking the fluorescence intensity (Ex: 488 nm, Em: 521 nm, Cutoff: 515 nm) using a Molecular Devices SpectraMax M2 microplate reader. Based on the results, titration curve was plotted (relative activities vs. CB[7] / NP molar ratio).

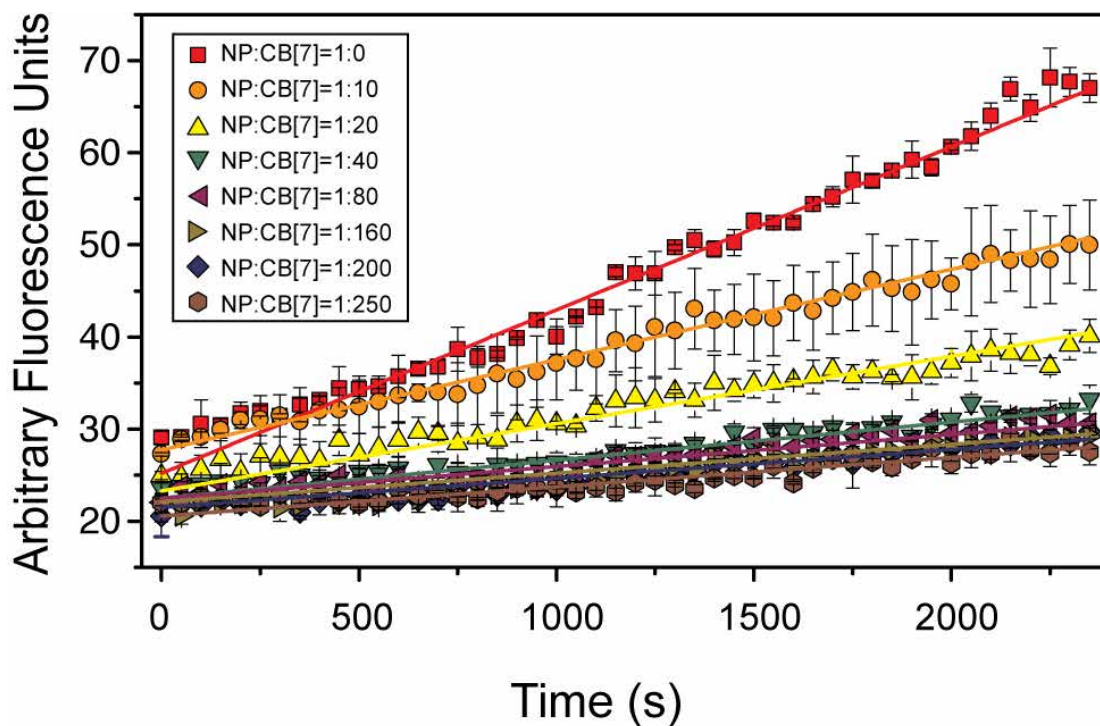


**Figure S19.** The dependence of reaction rate on the concentration of CB[7].

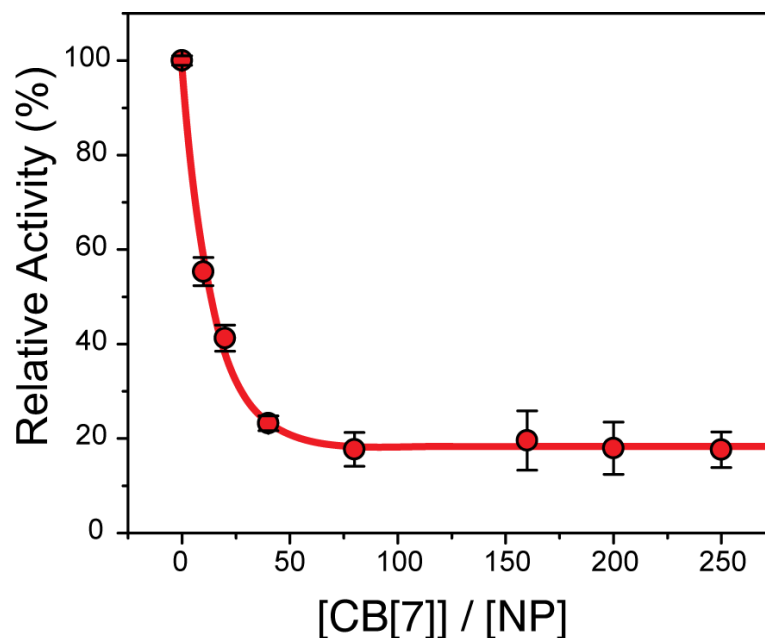


**Figure S20.** The reaction curve for relative activity versus [CB[7]]/[NP]

### **Inductively coupled plasma mass spectrometry (ICP-MS) instrumentation**

The ICP-MS analyses were performed on a Perkin-Elmer NexION 300X ICP mass spectrometer.  $^{197}\text{Au}$  and  $^{106}\text{Pd}$  were measured under the standard mode. Operating conditions are listed as below: nebulizer flow rate: 0.95 L/min; rf power: 1600 W; plasma Ar flow rate: 18 L/min; dwell time: 50 ms. Standard gold and palladium solutions (concentration: 0, 0.2, 0.5, 1, 2, 5, 10, and 20 ppb) were prepared for the quantification.

### **ICP-MS sample preparation for the quantification of gold and palladium**

0.5 mL of fresh *aqua regia* was added to the 10  $\mu\text{L}$  sample solution and then the sample was diluted to 10 mL with de-ionized water.

	Au	Pd	Pd ppb	Pd (ng)	Pd (ng)/ AuNP (pmol)	Pd (pmol)/ AuNP (pmol)
Sample 1	655784.588	21938.941	0.836205	8.219063	3.38	31.78
Sample 2	668543.332	22382.472	0.851752	8.537958	3.51	33.02
Sample 3	647151.360	23467.029	0.889766	9.186836	3.40	31.97
				Average	3.43	32.25
				S.D.	0.07	0.66

**Figure S21.** Palladium catalyst amount in the **NP\_Pd** nanozyme calculated using ICP-MS measurement.

### Catalytic activity of the nanozymes (NP\_Pd) inside vial

Catalytic activities of **NP\_Pd** and **NP\_Pd\_CB[7]** were tested in vials using 400 nM of **NP\_Pd** and 400 nM of **NP\_Pd\_CB[7]** in 2 ml of DI water. 5  $\mu$ L of caged rhodamine 110 substrate (20 mM in DMSO) was added in these nanozyme solutions. Fluorescence was observed using the nanozymes (**NP\_Pd**) while only little background fluorescence that it is coming from the caged-fluorophore was observed with the **NP\_Pd\_CB[7]** at 6 h as shown in Figure S22.

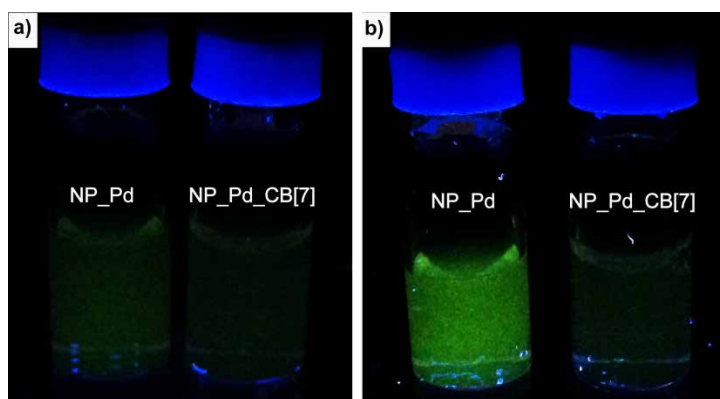


**Figure S22.** Photos of the reaction mixtures in water with **NP\_Pd** and **NP\_Pd\_CB[7]** under UV light at a, 0 h and b, 6 h.

## Kinetics studies of NP\_Pd and NP\_Pd\_CB[7] before and after ADA addition

Fluorescence was recorded using a Hewlett-Packard 8452A UV-Vis spectrophotometer. Experiment was performed in a 96 well plate with parameters were set to  $\lambda_{\text{ex}}=488$  nm,  $\lambda_{\text{em}}=530$  nm and  $\lambda_{\text{cutoff}}=515$  nm. 400 nM of **NP\_Pd** and 400 nM of **NP\_Pd\_CB[7]** were mixed with caged Rhodamine 110 (final concentration is 80  $\mu\text{M}$ ) in 200  $\mu\text{L}$  of DI water. Similar to **NP\_Ru**, in the presence of **NP\_Pd**, caged substrate started to be cleaved and an increase in fluorescence was observed. However, CB[7] complexation blocked the catalysis and no fluorescence was observed (Figure S23a). 40 minutes later, ADA with a final concentration of 0.4 mM was added and fluorescence was read for another 40 minutes. After ADA addition, CB[7] decomplexed from nanozyme and catalysis was restored (Figure S23b). Measurements were done in triplicate. Error bars represent the standard deviations of these measurements.

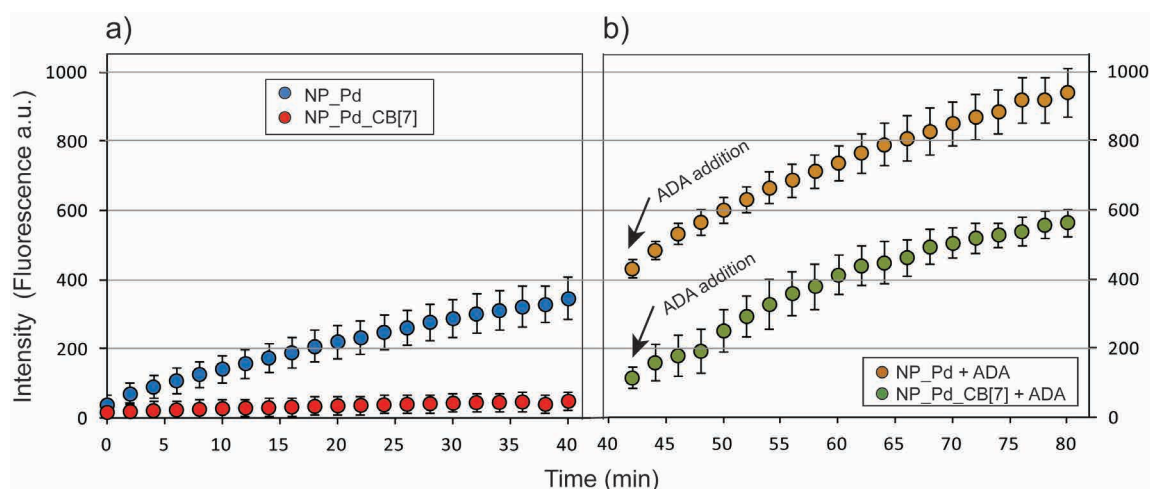


**Figure S23.** Kinetics of palladium catalyst embedded nanozymes. Fluorescence generation by **NP\_Pd** and **NP\_Pd\_CB[7]** a, before ADA addition and b, after ADA addition.

## Cellular uptake of the nanozymes with and without CB[7] tracked by ICP-MS

ICP-MS measurements were performed on a Perkin Elmer Elan 6100. Operating conditions of the ICP-MS are listed below: RF power: 1200 W; plasma Ar flow rate: 15 L/min; nebulizer Ar flow rate: 0.96 L/min; isotopes monitored: 197Au; dwell time: 50 ms; nebulizer: cross flow; spray chamber: Scott. Nanozyme (**NP\_Ru**) and **NP\_Ru\_CB[7]** (0.2  $\mu\text{M}$ ) was incubated with pre seeded HeLa cells in 24 well plates (20,000 cells/well) for 24 h. After 24 h incubation, old media were removed and cells were washed three times with PBS (500  $\mu\text{L}$ ). Then lysis buffer (300  $\mu\text{L}$ ) was added to the cells. The resulting cell lysate was digested overnight using  $\text{HNO}_3$  and  $\text{H}_2\text{O}_2$  (3:1 ml). On the following day, aqua regia (3 mL)

was added, and then the sample was allowed to react for another 2-3 h. The sample solution was then diluted to 10 mL with deionized water and aqua regia with the final solution containing 5% aqua regia. The gold nanoparticle sample solution was measured by ICP-MS under the operating conditions described above. Cellular uptake experiments with each gold nanoparticle were repeated in triplicate, and each replicate was measured 5 times by ICP-MS. A series of gold standard solutions (20, 10, 5, 2, 1, 0.5, 0.2, 0 ppb) containing 5% aqua regia were prepared before each experiment. The resulting calibration line was used to determine amount of gold taken up by cells.

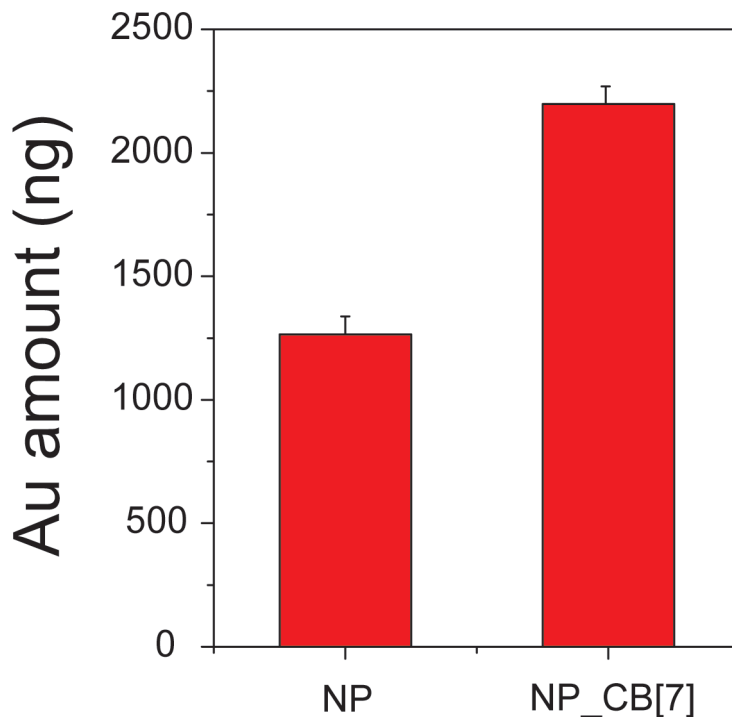


**Figure S24.** Nanozyme uptake assay by tracking the gold amount through ICP-MS.

### Cell viability assay

Toxicity of nanozyme (**NP\_Ru**) and only **NP** were checked using alamar blue assay. HeLa cells were grown in a cell culture flask using low-glucose Dulbecco's modified Eagle medium (DMEM) supplemented with 10% fetal bovine serum at 37°C in a humidified atmosphere of 5% CO<sub>2</sub>. When cells were more than 80% confluent, HeLa cells were seeded at 10,000 cells in 200 µL per well in 96-well plates 24 h prior to the experiment. During the experiment old media were removed and cells were washed with 200 µL PBS once. Then, cells were treated

in triplicate with 200  $\mu$ L of nanozyme (**NP\_Ru**) or only **NP** with different concentrations (10, 50, 100, 200 nM). After 24 h cells were washed with 200  $\mu$ L PBS three times and treated with 200  $\mu$ L of alamar blue solution in DMEM (10% solution) for 3 h. Cell viability was monitored by alamar blue assay (Ex: 460 nm, Em: 490 nm, Cutoff: 470 nm) using a Molecular Devices SpectraMax M2 microplate reader. Results demonstrated that both nanozyme (**NP\_Ru**) and **NP** showed high cell viability.

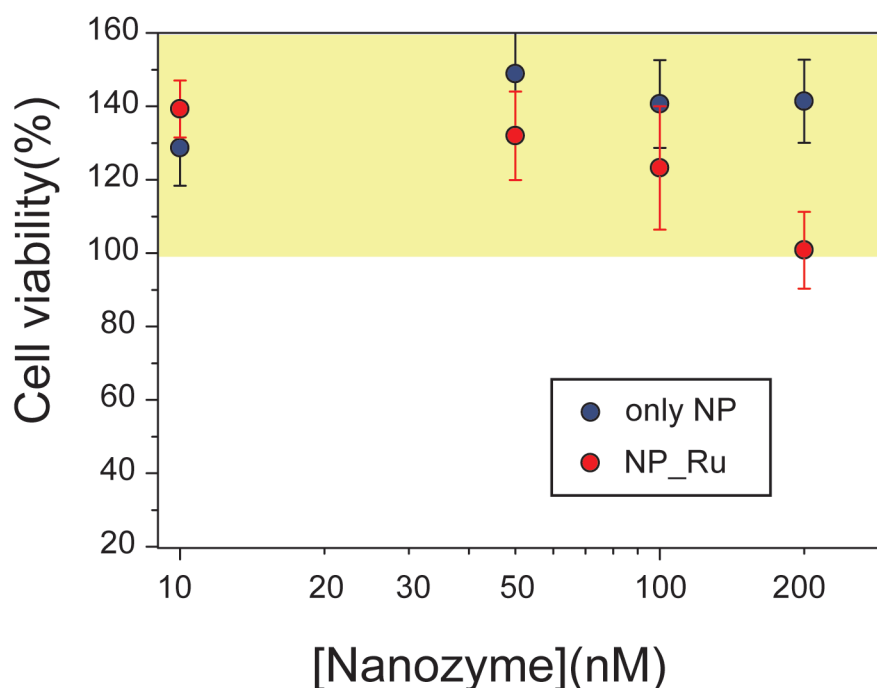


**Figure S25.** Cytotoxicity of the **NP\_Ru** and **NP** at various concentrations

### **Confocal microscopy with LysoTracker®**

Confocal microscopy images were obtained on a Zeiss LSM 510 Meta microscope by using a 63 $\times$  objective. The settings of the confocal microscope were as follows: green channel:  $\lambda_{ex}$ =488 nm and  $\lambda_{em}$ =BP 505-530 nm; red channel:  $\lambda_{ex}$ =543 nm and  $\lambda_{em}$ =LP 650 nm. Emission filters: BP=band pass, LP=high pass. LysoTracker® Red DND-99 (Invitrogen, 100 nM in 0.5 ml DMEM medium) was treated to cells for 30 min prior to the microscopy experiments.



Then cells were washed three times with PBS (0.5 mL) and images are taken when cells were in PBS.

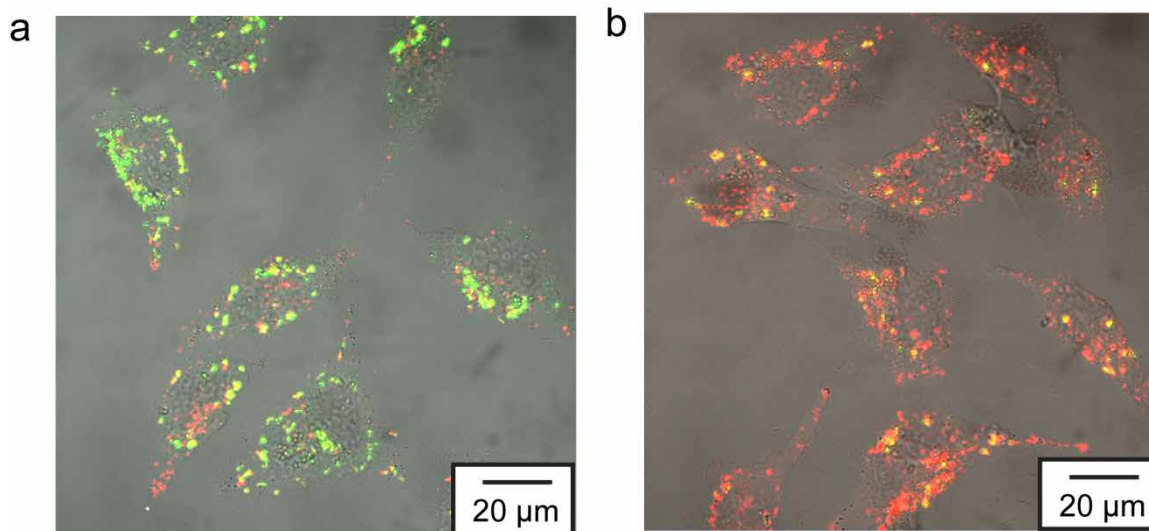


**Figure S26.** The confocal images of the cell treated with a, the nanozyme, substrate, and lysotracker; b, the nanozyme-bound-CB[7], substrate, ADA, and lysotracker.

### **Complexation of free CB[7] with NP\_Ru nanozyme and inhibiting the catalysis**

HeLa cells were seeded at 80,000 cells (1 ml serum containing media) in confocal dish 24 h prior to the experiment. Old media were replaced by 200 nM of the **NP\_Ru** nanozymes and the cells were incubated for 24 h and washed with PBS buffer three times. Some of the confocal dishes that were incubated with **NP\_Ru** were treated with free CB[7] (40 μM, 1 mL) while the rest was treated with only serum containing media. After 24 h, cells were washed with PBS three times and were incubated with 100 μM of the substrates for 24 h. Confocal microscope images showed a significant decrease in the fluorescence when cells were treated with free CB[7] solution before the addition of substrate. This



observation verified the complexation of CB[7] to **NP\_Ru** nanozyme and blocking the catalysis.

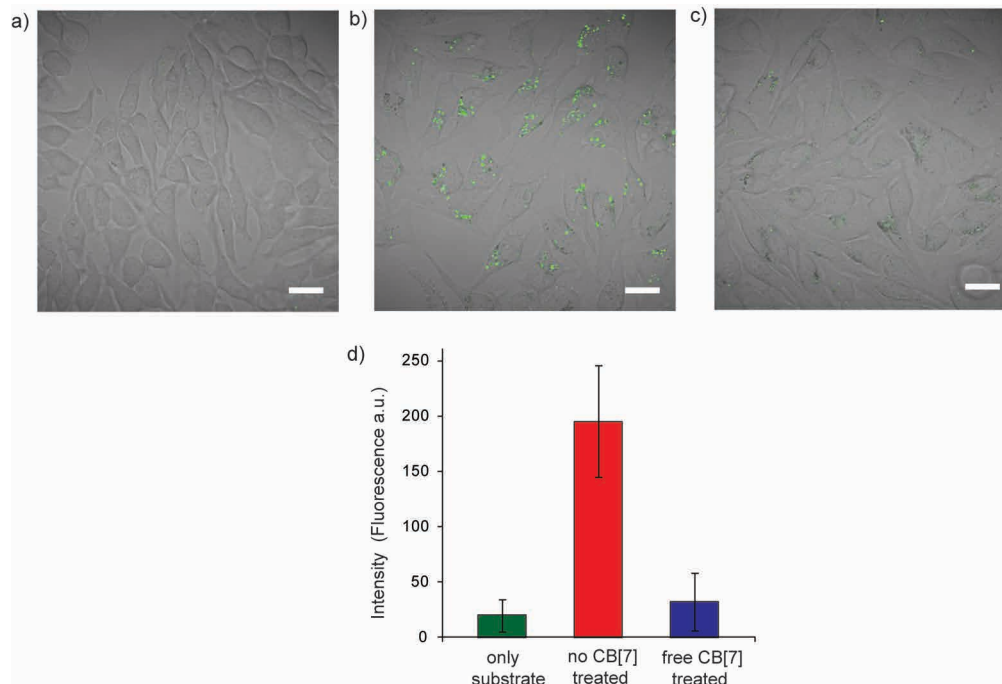


**Figure S27.** Confocal microscopy images of HeLa cells incubated with only substrate (a), **NP\_Ru** + substrate (b), and **NP\_Ru** nanozyme + free CB[7] + substrate (c) (scale bars = 20  $\mu$ m). Fluorescence intensities were obtained from confocal images using ImageJ program (d).

### Intracellular gating of the nanozyme using palladium catalyst

HeLa cells were seeded at 80,000 cells in 1 mL in confocal dish 24 h prior to the experiment. During the experiment old media were replaced by 100 nM of the nanozymes and the nanozyme-bound CB[7] in serum-containing media and the cells were incubated for 24 h and washed with PBS buffer three times. 100  $\mu$ M of the substrates were then added to the cells and incubated for 24 h. The cells were then washed with PBS three times. In the case of ADA treatment, cells were treated with 0.4 mM ADA solution (0.5 mL) for 24 h. Confocal microscopy images

were obtained on a Zeiss LSM 510 Meta microscope by using a 63× objective. The settings of the confocal microscope were as follows: green channel:  $\lambda_{ex}$ =488 nm and  $\lambda_{em}$ =BP 505-530 nm; red channel:  $\lambda_{ex}$ =543 nm and  $\lambda_{em}$ =LP 650 nm. Emission filters: BP=band pass, LP=high pass.

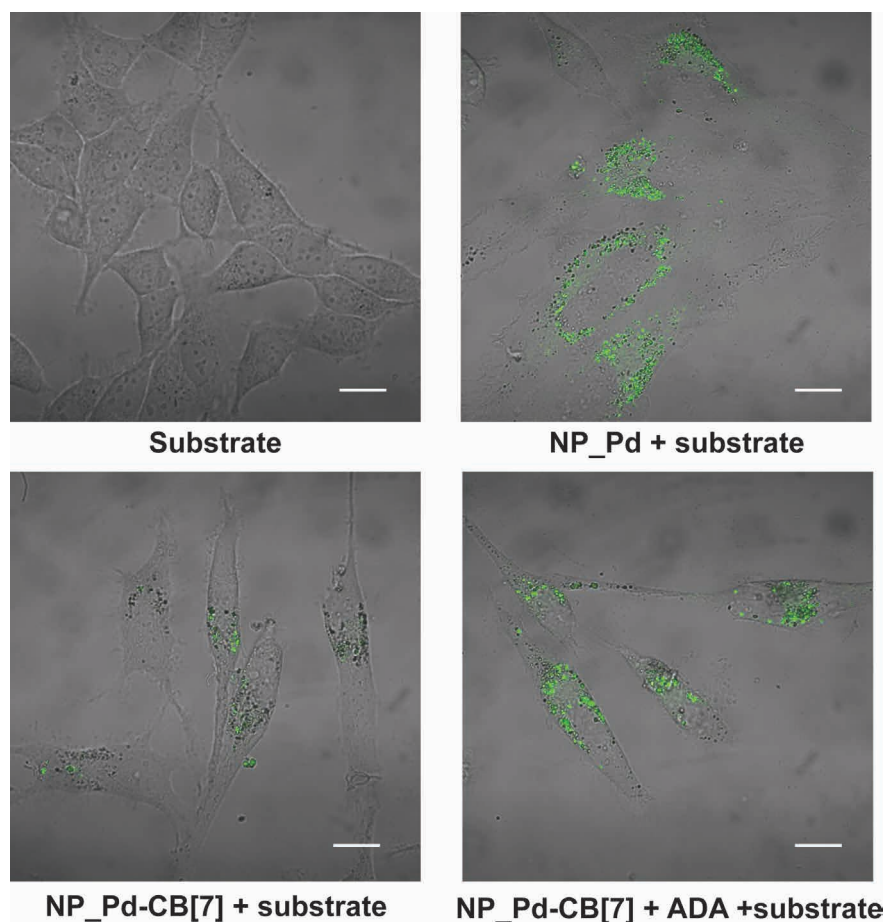


**Figure S28.** Intracellular gated-catalysis using NP\_Pd/NP\_Pd\_CB[7] (scale bars = 10  $\mu$ m).

### **Monitoring the cleavage of propargyl by NP-Pd using Matrix-assisted laser desorption/ionization (MALDI)-MS**

1 mM of pro-5FU was mixed with 100 nM **NP\_Pd** in DI water for 15, 48, and 72 h.

Results revealed that after 15 h almost 50 % cleavage was observed while after 72 h minimal amounts of pro-5FU detected.

#### **MALDI-MS analysis:**

200  $\mu$ L of the sample was filtered by 10K molecular weight cut off filter at 14,000 rpm for 15 minutes. A saturated solution of matrix  $\alpha$ -cyano-4-hydroxycinnamic acid ( $\alpha$ -CHCA) solution was prepared in 70% acetonitrile and 30% water. The filtered sample was mixed with the matrix solution in 1:1 ratio. 2  $\mu$ L of the mixture was spotted on a stainless steel MALDI-MS sample carrier. The spot was air dried before analysis. The samples were characterized by Bruker Autoflex III MALDI-TOF MS. The laser power was optimized to 80%. A total of 200 laser shots were fired per measurement. Data processing was performed using Bruker flex Analysis (version 3.3) software. The procedure was repeated for 3 consecutive days to check the conversion of prodrug to drug.

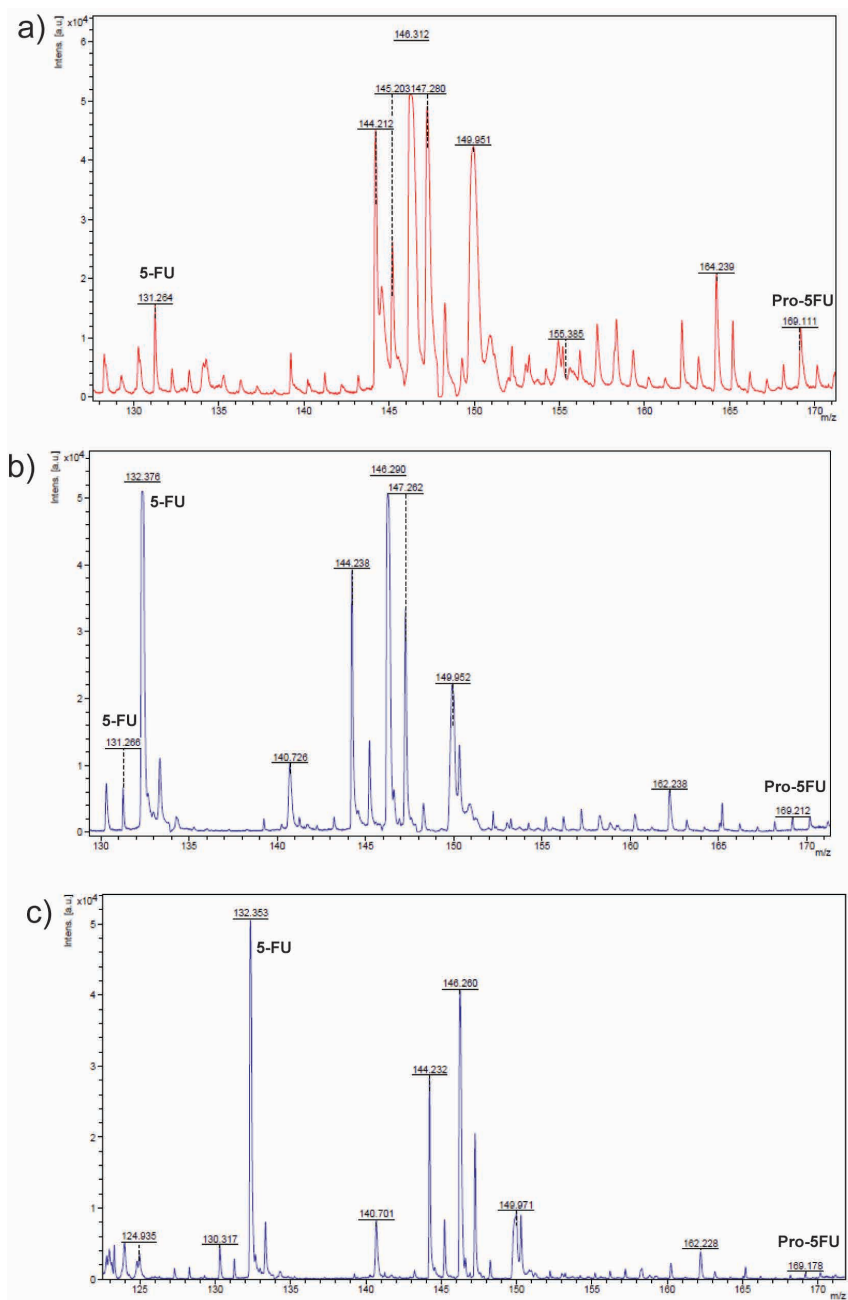


**Figure S29.** Cleavage of propargyl functionality of prodrug was monitored using MALDI-MS at (a) 15, (b) 48, and (c) 72 h.

### Rhodamine 110 fluorescence standard curve

We can estimate the concentration of the product after catalytic reaction, using the fluorescence intensity coming from rhodamine 110 product. For this purpose, a fluorescence standard curve for rhodamine 110 was obtained. The stock solution of rhodamine 110 (0.3 mM, 1 mL) was prepared in water. Successive dilutions were done, and the fluorescence intensity of prepared solutions (0.03, 0.06, 0.15, 0.3, 0.6, 1.2, 1.8, 2.4  $\mu\text{M}$ ) were directly measured by microplate reader (SpectraMax M2). The obtained curve slope is  $1.9 \times 10^3$  a.u. /  $\mu\text{M}$ .

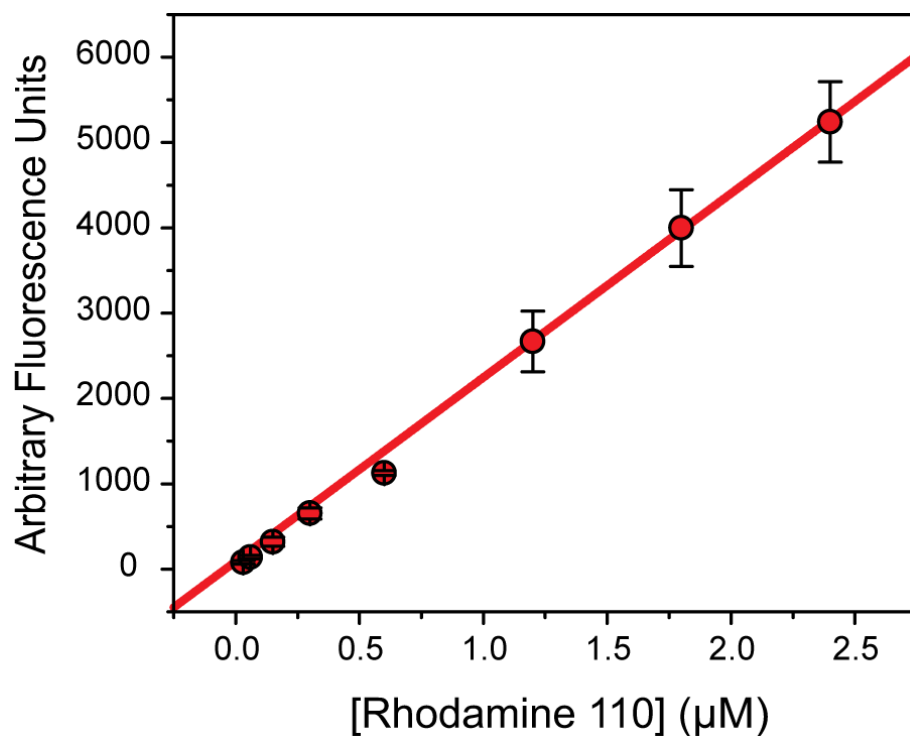


**Figure 30.** The standard curve of the rhodamine 110 prepared for the calculation of the reaction rate.

## References

---

1. Kanaras, A. G., Kamounah, F. S., Schaumburg, K., Kiely, C. J. & Brust, M. Thioalkylated tetraethylene glycol: a new ligand for water soluble monolayer protected gold clusters. *Chem. Commun.* 2294–2295 (2002).
2. Brust, M., Walker, M., Bethell, D. & Schiffrin, D. J. Synthesis of thiol-derivatised gold nanoparticles in a two-phase liquid–liquid system. *J. Chem. Soc. Chem. Commun.* 801-802 (1994).
3. Templeton, A. C., Wuelfing, W. P. & Murray, R. W. Monolayer-Protected Cluster Molecules. *Acc. Chem. Res.* **33**, 27–36 (2000).
4. Yan, B. *et al.* Laser desorption/ionization mass spectrometry analysis of monolayer-protected gold nanoparticles. *Anal. Bioanal. Chem.* **396**, 1025–1035 (2009).